



PAPER • OPEN ACCESS

Variations in size-specific effective dose with patient stature and beam width for kV cone beam CT imaging in radiotherapy

To cite this article: C J Martin and A Abuhaimeed 2022 *J. Radiol. Prot.* **42** 031512

View the [article online](#) for updates and enhancements.

You may also like



- [Highly Enhanced TMR Ratio and for Double MgO-Based p-Mtj Spin-Valves with Top Co₂Fe₃B₂ Free Layer By Nanoscale-Thick Iron Diffusion-Barrier](#)
Seung-Eun Lee, Jong-Ung Baek, Tae-Hun Shim et al.
- [CT scanner-specific organ dose coefficients generated by Monte Carlo calculation for the ICRP adult male and female reference computational phantoms](#)
Jan TM Jansen, Paul C Shrimpton and Sue Edyvean
- [What is Nanotechnology?](#)



PAPER

OPEN ACCESS

Variations in size-specific effective dose with patient stature and beam width for kV cone beam CT imaging in radiotherapy

RECEIVED
3 May 2022REVISED
9 July 2022ACCEPTED FOR PUBLICATION
2 August 2022PUBLISHED
7 September 2022C J Martin^{1,*}  and A Abuhaimeed² ¹ Department of Clinical Physics and Bioengineering, University of Glasgow, Gartnavel Royal Hospital, Glasgow G12 0XH, United Kingdom² King Abdulaziz City for Science and Technology (KACST), Riyadh, Saudi Arabia

* Author to whom any correspondence should be addressed.

E-mail: colin.j.martin@ntlworld.com**Keywords:** cone beam CT (CBCT), radiotherapy, image guided radiation therapy (IGRT), image optimisation, size specific effective dose, patient dosimetry, Monte Carlo simulations

Original content from this work may be used under the terms of the [Creative Commons Attribution 4.0 licence](https://creativecommons.org/licenses/by/4.0/).

Any further distribution of this work must maintain attribution to the author(s) and the title of the work, journal citation and DOI.

**Abstract**

The facilities now available on linear accelerators for external beam radiotherapy enable radiation fields to be conformed to the shapes of tumours with a high level of precision. However, in order for the treatment delivered to take advantage of this, the patient must be positioned on the couch with the same degree of accuracy. Kilovoltage cone beam computed tomography systems are now incorporated into radiotherapy linear accelerators to allow imaging to be performed at the time of treatment, and image-guided radiation therapy is now standard in most radiotherapy departments throughout the world. However, because doses from imaging are much lower than therapy doses, less effort has been put into optimising radiological protection of imaging protocols. Standard imaging protocols supplied by the equipment vendor are often used with little adaptation to the stature of individual patients, and exposure factors and field sizes are frequently larger than necessary. In this study, the impact of using standard protocols for imaging anatomical phantoms of varying size from a library of 193 adult phantoms has been evaluated. Monte Carlo simulations were used to calculate doses for organs and tissues for each phantom, and results combined in terms of size-specific effective dose (SED). Values of SED from pelvic scans ranged from 11 mSv to 22 mSv for male phantoms and 8 mSv to 18 mSv for female phantoms, and for chest scans from 3.8 mSv to 7.6 mSv for male phantoms and 4.6 mSv to 9.5 mSv for female phantoms. Analysis of the results showed that if the same exposure parameters and field sizes are used, a person who is 5 cm shorter will receive a size SED that is 3%–10% greater, while a person who is 10 kg lighter will receive a dose that is 10%–14% greater compared with the average size.

1. Introduction**1.1. Image-guided radiation therapy**

External beam radiation therapy aims to give a radiation dose to the tumour that is high enough to kill all cancer cells while keeping doses to normal healthy tissues low enough to minimise the risk of serious health consequences. In current linear accelerators (linacs) used for treatments, the radiation beams are conformed to the shape of the tumour using multi-leaf collimators (MLCs) with individually adjustable tungsten alloy leaves. Beams are delivered from multiple directions with new techniques that enable dose distributions to be conformed effectively to the tumour volume. These techniques include intensity-modulated radiation therapy, which involves adjusting the MLC leaves while x-rays are being produced, volumetric-modulated arc therapy, in which the treatment head is moved in arcs around the patient while the beam shape and dose are changed automatically [1–3], and stereotactic body radiotherapy, in which higher doses and smaller treatment beams are directed from many different angles [4, 5].

Three-dimensional computed tomography (CT) images of a patient form the basis of the plan for the treatment that will be prepared by a dedicated computer planning system. The position of the tumour is

identified with respect to anatomical or other landmarks on the patient, but the treatment will only be effective if the radiation can be delivered with a high degree of accuracy. In order to take full advantage of all the improvements offered by the new techniques, patients must be positioned consistently to the nearest millimetre, and even sub-millimetre levels. This is almost impossible without carrying out additional imaging at the time of treatment delivery to confirm that the tumour target is positioned accurately with respect to the treatment beams. Imaging is often performed at the start of each fraction and comparisons made with the treatment plan and planning images. Without this, errors in patient positioning with respect to the treatment plan would be replicated throughout the treatment process, and these, together with any random errors in positioning of patients at each fraction, could compromise success of the treatment.

The process of repeating imaging through the course of a treatment is referred to as image-guided radiation therapy (IGRT) [6–8]. Modern linacs incorporate kilovoltage (kV) imaging systems with flat panel detectors that can be used either to take planar radiographs or, by rotating the x-ray tube and detector around the patient, cone beam CT (CBCT) scans [9]. Radiotherapy linacs with kV CBCT imaging are now widely used throughout the world and are purchased routinely when older treatment machines are replaced. The improvements in accuracy of localisation achieved through performance of IGRT at the time of treatment allow higher doses to be given to the tumour without increasing doses to surrounding tissues. However, successful delivery of radiation treatment requires planning images with the tumour position identified with respect to anatomical references or fiducial markers, which must be located within the field being imaged during the course of treatment. Therefore, the imaging field is generally considerably larger than the high-dose treatment field.

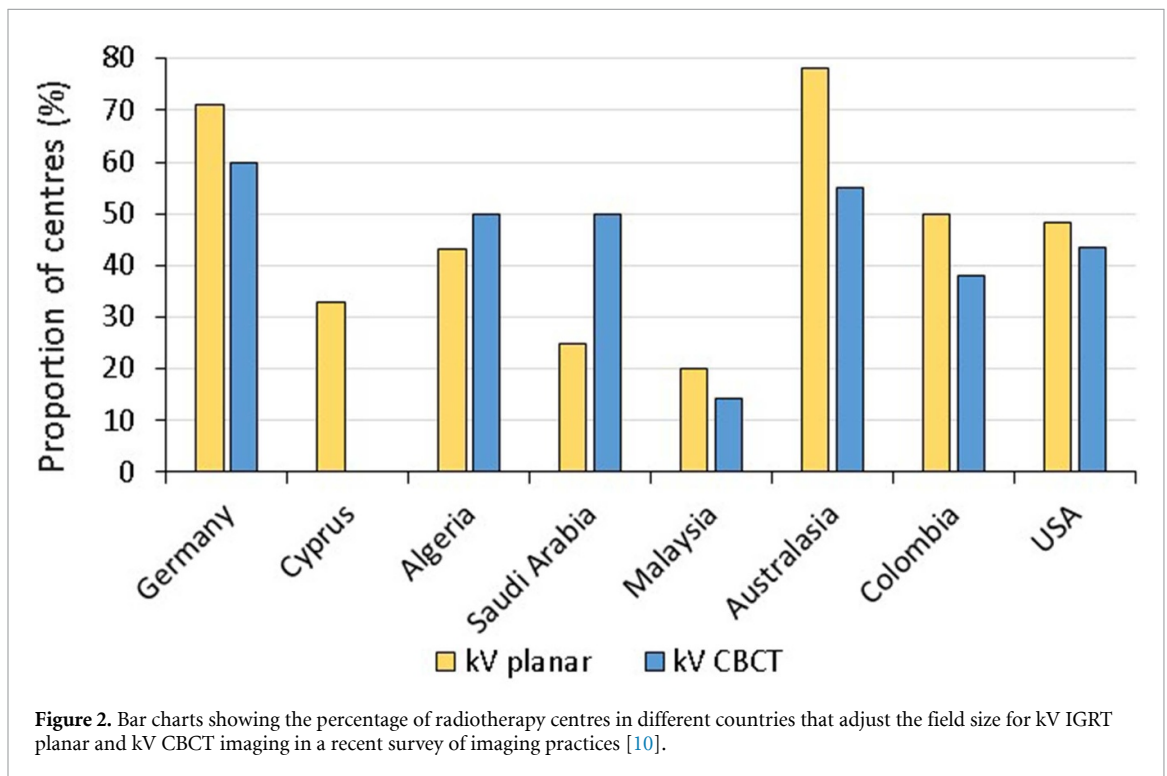
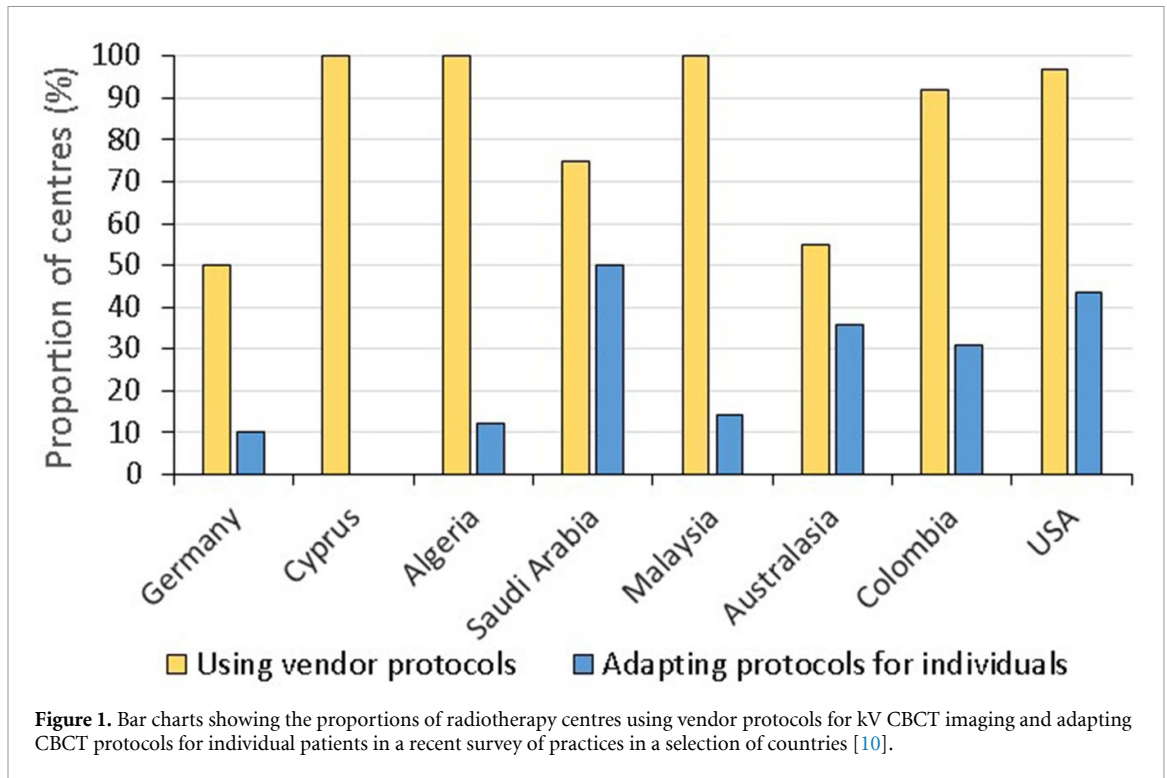
1.2. Practices in the use of imaging during radiotherapy treatment

A survey was carried out recently in radiotherapy centres in a selection of countries from around the world through the International Commission on Radiological Protection (ICRP) mentee programme to assess imaging practices in radiotherapy; the methods are described in Martin *et al* [10]. The survey indicated that almost all centres used CBCT and that it was the most important imaging tool used during the treatment cycle. The ICRP survey sought information on the use of imaging during radiotherapy and included questions about the use of CBCT protocols supplied by the equipment vendor and the amount of optimisation undertaken for individual patients. The imaging modality applied most widely was kV CBCT, being used by all the radiotherapy centres in six of the nine countries surveyed and by 90% in two others. One country, which had the lowest value for the human development index, only had two centres with kV imaging capability and vendor protocols were used without adaptation in both; these data have not been included in the bar chart analysis. Among the centres that used CBCT, between 50% and 100% used standard imaging protocols supplied by the vendor and numbers of centres adapting protocols for individual patients through adjusting the exposure factors were in the minority (figure 1).

The use of standard exposure settings and field sizes for CBCT scans on most patients can result in more organs being exposed in smaller patients with higher doses. Only about half of the centres adjusted field sizes for planar kV imaging or adjusted the jaw blade settings determining the length of the body scanned in CBCT (figure 2). Since few radiotherapy centres recorded any dose information relating to imaging exposures, it is not possible to draw conclusions about patient dose levels at this stage. The present study using Monte Carlo simulations is being undertaken to give an indication of the dose savings that might be achieved through adjustment of exposure factors and field sizes for patient stature.

1.3. Potential doses from imaging

The doses from imaging are much smaller than those from treatment, and so they have been considered to be of little concern and less effort has been put into their reduction than in diagnostic x-ray imaging. However, ionising radiation is known to cause cancer [11, 12] and studies have suggested that doses delivered from CT scans for medical imaging are associated with a raised risk of cancer [13]. The recent changes in patterns of imaging have the potential to give much higher doses to patients. Measurements on phantoms with kV CBCT imaging systems show doses to individual organs can be tens of milligray [14, 15]. If CBCT scans are performed during up to 30 fractions of an external beam treatment, doses can no longer be considered insignificant. This exposure is important to consider, since the imaging performed includes normal tissues surrounding the tumour, so contributing to risks of second cancers in adjacent organs and tissues [16–18]. Moreover, cancer patients may potentially have a higher genetic risk of tumour induction. Doses to tissues from repetitive imaging procedures over 1 Gy have been reported for some patients [19], and these patients may also have received more imaging procedures prior to treatment during investigation of their disease. Therefore, improvements in the accuracy with which boundaries of the tumour target, sparing normal tissues from exposure within the treatment beam, must be balanced against the additional radiation doses from imaging.



In diagnostic radiology procedures, exposure factors and settings are adjusted for individual patients, but this is often not the case in radiotherapy. Many centres use protocols provided by equipment vendors without any adjustment, and training of radiotherapy staff may not include techniques for optimisation of the imaging dose [20–22]. Limiting the size of the field being imaged will reduce the volume of tissue exposed and may allow irradiation of some sensitive organs to be avoided altogether [23]. The present study uses Monte Carlo simulations of anatomical phantoms of varying size, for which values of the size-specific effective dose (SED) are derived [24]. These are used to investigate the magnitudes of dose variations when standard exposure settings and beam widths are used for imaging phantoms of varying stature. From this, the dose savings that could be achieved through optimisation of radiological protection are evaluated.

2. Methods

There are two major vendors of linacs fitted with kV imaging systems; Varian and Elekta, and this study concentrates on the Varian system. In order to investigate the magnitudes of higher dose levels that might result from using standard CBCT protocols for individual patients, CBCT exposures were simulated on anatomical phantoms of varying size using the BEAMnrc/EGSnrc Monte Carlo code developed to represent the kV imaging system on a Varian Truebeam linear accelerator [25–27]. Imaging procedures for the chest and pelvis were simulated, using the half-fan mode with 360° rotation, 120 kV and a range of widths for the cone beam from 18 cm to 26 cm. Organ, tissue and SEDs have been calculated per 100 mAs [28, 29]. However, values used for scans based on clinical protocols are 270 mAs for the chest and over 1080 mAs for the pelvis [28].

Organ and tissue doses were evaluated using the DOSXYZnrc/EGSnrc code [30, 31] on a library of computational human phantoms known as PHANTOMS, which has been developed by the National Cancer Institute of the National Institutes of Health in the United States and contains 193 adult male and female phantoms [32–35]. Simulations were carried out for all the phantoms and results selected for groupings within certain ranges of body mass index (BMI). The library contains phantoms based on reconstructed CT images of patients who had undergone CT scans. The heights for female phantoms cover the range 150–175 cm with weights up to 135 kg for the 165 cm phantom, and for male phantoms the range is 160–190 cm with weights up to 140 kg for the 180 cm phantom. For each phantom height, there are ranges in weight at 5 kg intervals, with a range of 40–95 kg for the shortest female phantom and 50–95 kg for the shortest male phantom.

Output files of the simulations were analysed using a MATLAB code developed in house for this purpose. The organ and tissue doses were normalised with respect to an exposure of 100 mAs and values for scans of each phantom were determined from the code and combined through the equation used to derive effective dose to calculate the SED [29]

$$\text{SED} = \sum_T w_T H_T \quad (1)$$

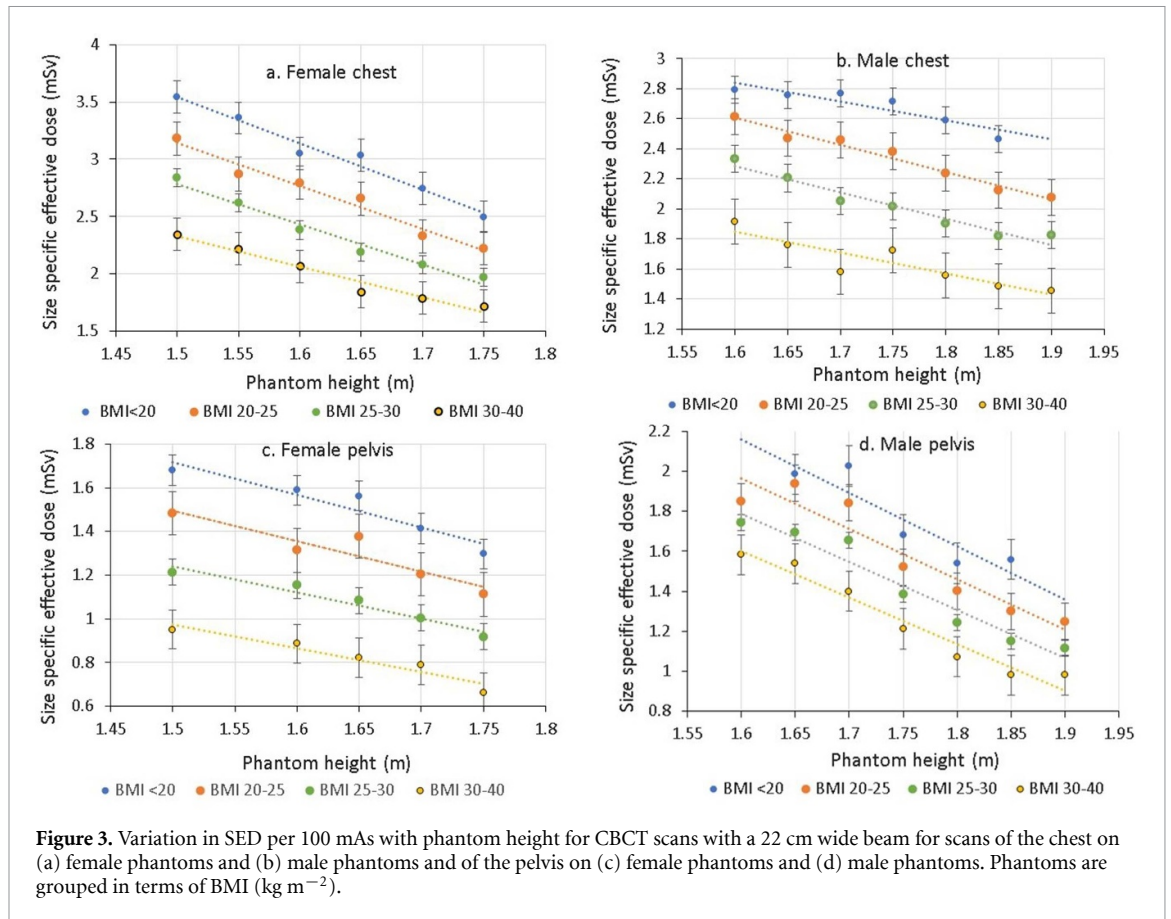
where H_T is the equivalent dose to organ or tissue T , and w_T is the corresponding tissue weighting factor according to ICRP 103 [11]. Calculations were performed for male and female phantoms separately.

The use of a SED allows doses for individuals of different statures to be compared in a manner that gives an indication of relative risk. Organ doses for the prostate and testes are included for the male phantoms and ovaries and uterus for female phantoms. However, having phantoms with many different heights and weights leads to variations in phantom thickness that are not correlated with either measurement. In order to compare doses for phantoms of varying height, phantoms were grouped in terms of BMI to allow individuals of comparable build to be matched for assessing the influence of beam width and height on doses to individual organs and SED. The BMI is equal to weight in kilogrammes divided by the square of the height in metres, and values between 20 and 25 kg m⁻² are considered to represent the normal range. Phantom data were put into groups representing ranges of 17–20 kg m⁻² (underweight), 20–25 kg m⁻² (normal), 25–30 kg m⁻² (overweight) and 30–40 kg m⁻² (obese). Simulations were carried out for all the adult phantoms in the library, but the numbers of individuals in the lower weight groups were more limited. As a result, for specific imaging arrangements with a particular beam width there were generally two phantoms in the 17–20 kg m⁻² group, three or four in the 20–25 kg m⁻² and 25–30 kg m⁻² groups, and six or seven in the 30–40 kg m⁻² group.

3. Results

3.1. Variations in CBCT doses with phantom height

A beam width representing an average for values used by different vendors for routine CBCT imaging is 22 cm, so values of SED were calculated with this beam width for all adult phantoms in the library covering the full range of heights. Results are plotted against phantom/patient height for the different groupings of BMI (kg m⁻²) in figure 3 for chest and pelvis imaging procedures on male and female phantoms. The error bars represent the standard deviations of results from the phantoms within each BMI group, except for the lowest BMI groupings in which there were sometimes only two individuals because of the limitation from the range of phantom sizes available. In this case, the bar simply represents the difference between the two values. The ranges in SED per 100 mAs for chest scans of 1.7–3.5 mSv for female phantoms and 1.4–2.8 mSv for male phantoms equate to values for scans performed in the clinic using 270 mAs of 4.6–9.5 mSv for women and 3.8–7.6 mSv for men. The ranges in SED per 100 mAs for pelvis scans of 0.7–1.7 mSv for female



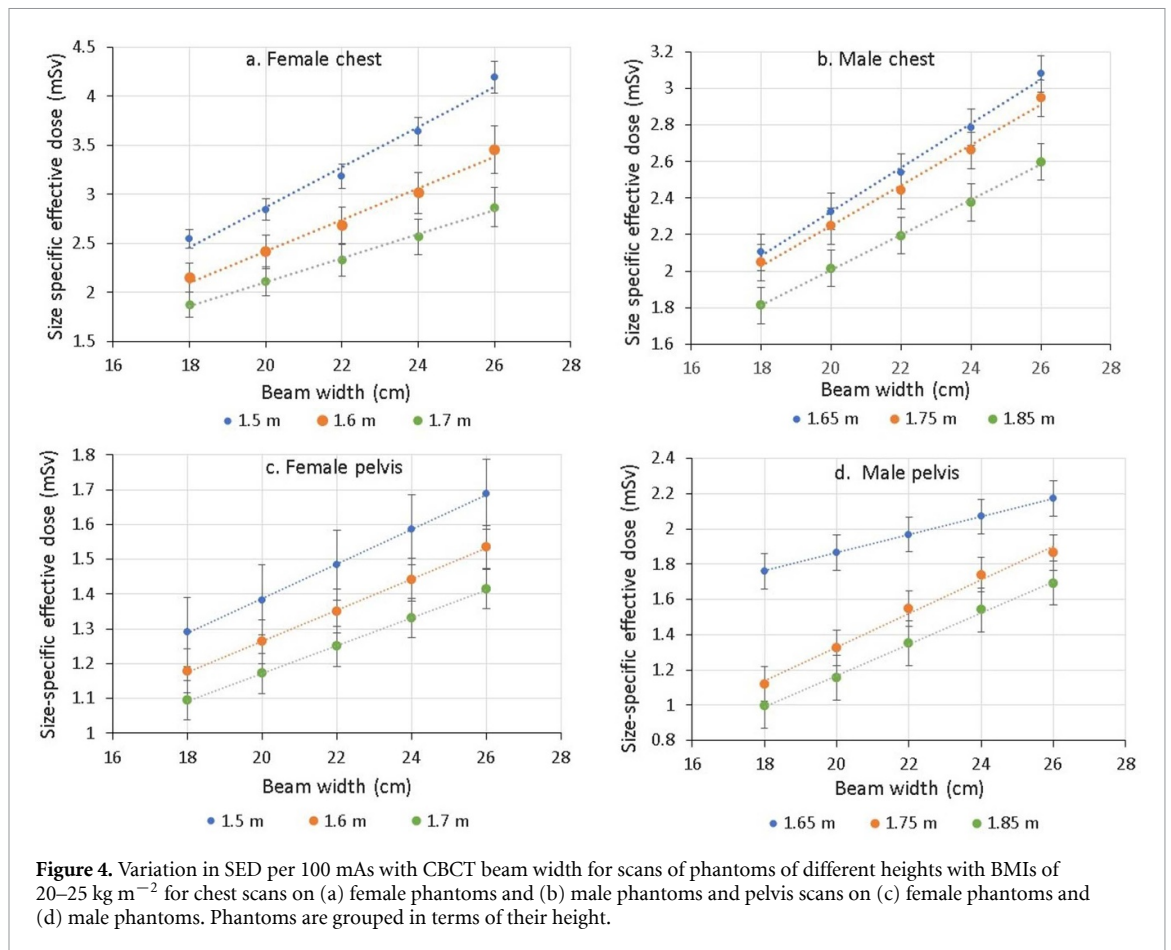
phantoms and 1–2 mSv for male phantoms equate to values for scans performed in the clinic using 1080 mAs of 8–18 mSv for women and 11–22 mSv for men.

The SED declined steadily with phantom height, as the proportions of some organs and tissues within the primary beam declined. The SED for a chest scan on a female phantom that was 5 cm shorter being 5%–7% higher, and that for a 5 cm shorter male phantom being 3%–5% higher. While for scans of the pelvis, the dose to a female phantom that was 5 cm shorter was 4%–6% higher, and that for a shorter male phantom it was 7%–10% higher. The dose was lower for phantoms with a higher BMI, as organs were protected to some degree by overlying tissues. In a similar manner, plots of SED against beam width (figure 4) show that the shorter phantoms would receive higher doses. The SED increases with beam width as larger proportions of some organs are brought within the primary beam, with a 2 cm increase in beam width for chest scans resulting in a 10%–12% increase in SED for a female phantom and a 9% increase for a male phantom, while a 2 cm increase in beam width for pelvis scans results in a 6%–7% increase in SED for a female phantom and an 11%–13% for taller male phantoms, but only a 5% increase for the 165 cm tall male phantom.

Doses decline in taller phantoms and the rates of decline vary, depending on the positions of each organ within the scanned region and the portions lying within or outside the main beam. The dose to the thyroid, being a small organ on the edge of the scan field, will decline rapidly for CBCT scans of the chest as beam width is reduced. The thyroid dose will be smaller in taller phantoms, and having its own tissue weighting factor will reduce the SED for a chest CBCT substantially for tall patients. Doses to larger organs in the chest occupying a substantial proportion of the part of the body imaged will decline more slowly with beam width or patient height. In a similar manner for pelvis scans, the testes in male phantoms represent a small organ on the edge of the scan field, for which the dose will decline rapidly as beam width is reduced. As a result, changes in SED with height (figure 3(d)) or beam width (figure 4(d)) are more rapid in the male phantoms, because the CBCT beam will cover an increasing volume of the testes. The change is less for the shorter phantoms, as the testes lie within the x-ray beam for most beam widths.

3.2. Variations in dose with phantom weight

Values of the SED for phantoms of specific heights being imaged with a 22 cm wide beam are plotted against phantom weight in figure 5. These show a steady decline in dose per mAs as weight increases. The relationships between dose and weight for the male and female chest data sets and the female pelvis were

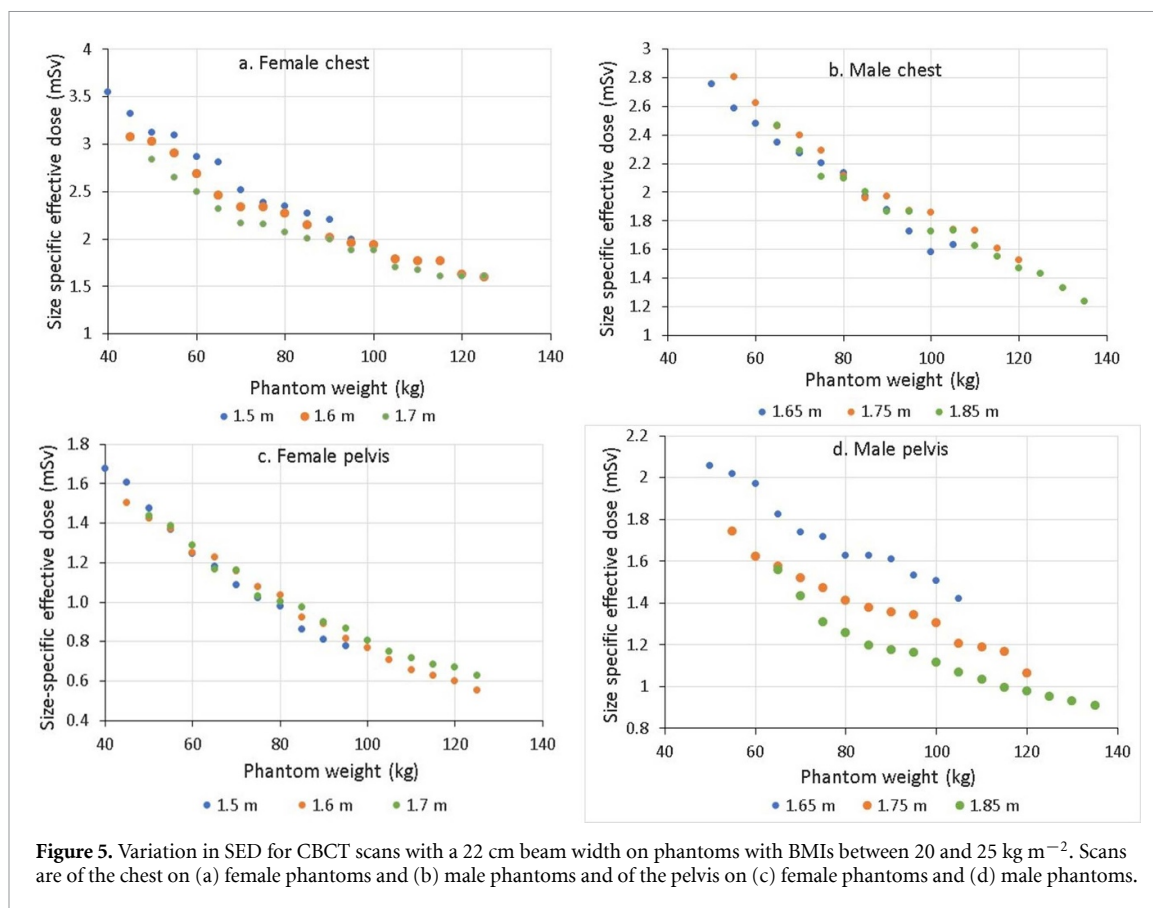


similar for phantoms of different heights. However, the plots of male pelvis scan doses for phantoms of different heights were more widely separated, with those for shorter phantoms having higher doses. This is primarily due to the inclusion of a greater proportion of the testes in the beam for the shorter phantoms.

A female patient whose weight is 60 kg will receive a SED that is 14% greater for a chest scan than one who is 70 kg, and 13% greater for a pelvic scan if the exposure is not reduced to take account of the weight difference. A male patient who weighs 70 kg will receive a SED from a chest scan that is 11% higher than that for a patient who is 80 kg and the SED for a pelvis scan will be about 10% higher if exposure factors are not changed to account for the weight difference.

4. Discussion

Imaging at the time of treatment in radiotherapy has become crucial in order to ensure that patients are accurately positioned to receive radiation treatments to take advantage of shaping of dose distributions to tumour targets with millimetre accuracy. Vendors of linacs in which kV imaging facilities are installed supply standard protocols. The Truebeam reference manual does not give data on the sizes of patients to which these apply, but they might be regarded as equating to the ICRP reference phantoms that have weights and heights for an adult female of 60 kg and 1.63 m and for an adult male of 73 kg and 1.76 m, respectively [36]. A survey of imaging practices revealed that in many radiotherapy centres protocols are not adapted for individual patients (figures 1 and 2), so that radiation protection aspects are not optimised [10]. Results from the Monte Carlo simulations carried out in this study have compared values for SEDs between phantoms of different stature. This shows that patients who are shorter or lighter will receive significantly higher doses if similar exposure factors and field sizes are used for CBCT scans on all patients. A person who is 5 cm shorter will receive a SED that is 3%–7% greater for a chest scan and 4%–10% greater for a pelvis scan. A person who is 10 kg lighter will receive a dose that is 11%–14% greater for a chest scan and 10%–13% greater for a pelvis scan. The differences amount to 0.7 mSv to 1.6 mSv from one scan, but since radiotherapy treatments are often given in 20–30 fractions, the increase in cumulative dose can be significant if protocols are not optimised. The main concern will be for patients who are substantially smaller and lighter, which would include children if the same imaging protocols were used as for adult patients. For example, the dose to a



female patient who weighed 50 kg might be 30% greater than for a patient who weighed 70 kg using the same imaging protocol (figure 5).

The culture of adapting imaging exposure parameters and field sizes to individual patients is less well established in IGRT than in diagnostic radiology. The organs included in the scan field that will have a more significant influence on the SED are the smaller ones that lie near the edge of the field, such as the thyroid and the testes. Doses to the testes in the pelvis scan cause SEDs for men to rise more rapidly than those for women as the beam width is increased (figure 4(d)). If exposure of the thyroid or testes can be avoided then this may reduce the size-specific effective dose (SED) considerably. The stochastic risks for the thyroid and the testes both decline more rapidly with age [11], and so the use of accurate collimation is of more significance for younger patients.

The adaptation of imaging field sizes for individual patients is done routinely in diagnostic imaging departments, with the lengths of CT scans being set accurately based on a scan projection radiograph taken before the start of the scan. However, the facilities on radiotherapy CBCT equipment to limit field size are generally more restricted, with more limited beam width options available. Although radiographic images can be taken with kV systems on linacs, these are not generally used to set collimation for CBCT scans. As a result, accurate collimation to exclude organs on the scan periphery is more difficult. The use of radiographic images combined with more flexible collimator blade settings would facilitate more accurate setting of x-ray field limits. Larger CBCT scan fields are often necessary to allow the extent of structures that need to be protected from therapeutic irradiation to be determined. Extending the scan field towards the patient's head can include more vertebrae which provide markers for matching field positions. However, for cases treated with stereotactic ablative radiotherapy techniques targeting small tumours in the lung or prostate, fiducial markers can be inserted into the tumour and used for matching with a small field size.

There is a potential to make some adjustments for CBCT scanning systems on some linacs. A patient-specific field size applied with a Varian Truebeam CBCT system that used four dynamic blades and tube current modulation has been reported by Parsons and Robar [37]. In this system, the size of the scan field was adjusted based on a volume of interest specified in the treatment plan. The use of this system reduced the scan dose by up to 80% and enhanced the contrast-to-noise ratio by a factor of ~ 2.2 . The Elekta XVI system has a series of lead collimators with the lateral field width being set at small, medium or large and the axial extension specified in terms of a series of options of different length [38]. The choice of collimator is based on the clinical case and size of the patient, and can reduce the imaging dose for small patients or

patients with smaller tumours. Effective doses from Elekta XVI scans have been reported to vary over the ranges 0.64–7.88 mSv, and 0.16–7.60 mSv for chest and pelvis scans, respectively [39]. However, these options are not widely available and standard settings are used by the majority of radiotherapy centres.

This study has shown the variations in magnitude of SEDs that will be delivered by CBCT imaging during IGRT when imaging protocols are not adapted to individual patients. Many centres use protocols provided by equipment manufacturers, which are often not optimal, and training of radiotherapy staff may not include awareness of techniques for optimisation of imaging dose. The provision of training of staff in imaging techniques and optimisation of radiological protection needs to be expanded. An element that is missing at the present time in many parts of the world is any measure of the doses delivered by imaging in radiotherapy. In order for more attention to be placed on optimisation of imaging, operators need to be aware of dose levels delivered by their equipment so they can evaluate the impact of changes made to protocols. The measurable quantities used to assess doses from CT imaging (CT dose index and dose-length product) are different from those employed in radiotherapy, they are not displayed routinely on many CBCT units and few centres record them. Optimisation of radiological protection in diagnostic imaging has been driven forward through staff monitoring patient doses and undertaking audits. Patient dose audit is the process in which results of a survey of patient doses are compared against relevant standards set in terms of diagnostic reference levels [40]. Steps are now being taken to carry out such evaluations for IGRT, although results have so far only been published for planning exposures [22]. More information on dose levels for imaging in IGRT is required together with the impact on doses to patients.

5. Limitations of the study

This study has only included analysis of doses from CBCT imaging using an imaging system for one vendor (Varian). Nevertheless, it gives an indication of the differences in doses that might be delivered to patients of varying size when protocols are not optimised. However, protocols and imaging regimes for different vendors will vary and the level of dose reduction that could be achieved will depend on local practices. The x-ray field sizes used for the assessments were the ones employed as standard, but values were not determined directly from surveys of patient imaging practices. Therefore, the study does not include a direct evaluation of doses from exposures carried out on actual patients.

6. Conclusions

This study has evaluated doses for individuals of different stature, represented by computational phantoms based on real patient images. The results demonstrate that if all patients are imaged with standard protocols with similar exposure factors and field sizes for CBCT, patients who are either shorter or lighter will receive significantly higher doses. A person who is 5 cm smaller will receive a SED that is 3%–10% greater if the same field sizes are used. A person who is 10 kg lighter will receive a dose that is 10%–14% greater, depending on the part of the body and patient stature. Although not the subject of this study, such dose differences would be of particular significance for imaging of children if adult protocols were used. Since a survey of imaging practices has indicated that the majority of radiotherapy centres do not adapt protocols for individual patients, differences of this order are likely to occur in practice. These can amount to differences in SED of 0.3–2.0 mSv per scan, and such scans may be performed at up to 30 fractions for some radiotherapy treatments. There is a need to improve facilities for adjustment of CBCT beam widths and raise the awareness of radiotherapy imaging staff for the need to optimise these exposures.

Acknowledgments

The authors would like to thank the National Cancer Institute of the National Institutes of Health (NIH) in the United States for sharing the PHANTOMS library used in this study, and the supercomputing lab at King Abdullah University of Science and Technology (KAUST) for their permission to perform all Monte Carlo simulations on the supercomputer (Shaheen).

The authors also wish to thank the following participants in the ICRP mentorship programme: Abdel-Hai Benali, Mario Djukelic, Sebastien Gros, Maria Cristina Plazas d'Leon, Yiannis Roussakis and Hossam Ragab Shaaban for their assistance in obtaining data on imaging practices in radiotherapy departments in their countries.

ORCID iDs

C J Martin  <https://orcid.org/0000-0002-0784-9002>

A Abuhaimeid  <https://orcid.org/0000-0003-4635-2047>

References

- [1] Webb S 2003 The physical basis of IMRT and inverse planning *Br. J. Radiol.* **76** 678–89
- [2] Webb S 2005 Intensity-modulated radiation therapy (IMRT): a clinical reality for cancer treatment, ‘any fool can understand this’. The 2004 Silvanus Thompson Memorial Lecture *Br. J. Radiol.* **78** S64–S72
- [3] Otto K 2008 Volumetric modulated arc therapy: IMRT in a single gantry arc *Med. Phys.* **35** 310–7
- [4] Timmerman R D, Kavanagh B D, Cho L C, Papiez L and Xing L 2007 Stereotactic body radiation therapy in multiple organ sites *J. Clin. Oncol.* **25** 947–52
- [5] Ball D *et al* 2019 Stereotactic ablative radiotherapy versus standard radiotherapy in stage 1 non-small-cell lung cancer (TROC 09.02 CHISEL): a phase 3, open-label, randomised controlled trial *Lancet Oncol.* **20** 494–503
- [6] Dawson L A and Sharpe M B 2006 Image-guided radiotherapy: rationale, benefits, and limitations *Lancet Oncol.* **7** 848–58
- [7] Mackie T R *et al* 2003 Image guidance for precise conformal radiotherapy *Int. J. Radiat. Oncol. Biol. Phys.* **56** 89–105
- [8] Mundt A J and Roeske J C 2011 *Image Guided Radiation Therapy: A Clinical Perspective* (Shelton, CT: Peoples Medical Physics Publishing House)
- [9] ICRP 2015 Radiological protection in cone beam computed tomography (CBCT). ICRP Publication 129 *Ann. ICRP* **44**
- [10] Martin C J *et al* 2021 An international survey of imaging practices in radiotherapy *Phys. Med.* **90** 53–65
- [11] ICRP 2007 The 2007 recommendations of the International Commission on Radiological Protection. ICRP Publication 103 *Ann. ICRP* **37**
- [12] ICRP 2021 The use of dose quantities in radiological protection. Publication 147 *Ann. ICRP* **50**
- [13] Pearce M S *et al* 2012 Radiation exposure from CT scans in childhood and subsequent risk of leukaemia and brain tumours: a retrospective cohort study *Lancet* **380** 499–505
- [14] Alaei P and Spezi E 2015 Imaging dose from cone beam computed tomography in radiation therapy *Phys. Med.* **31** 647–58
- [15] Abuhaimeid A, Martin C J and Sankaralingam M 2018 A Monte Carlo study of organ and effective doses of cone beam computed tomography (CBCT) scans in radiotherapy *J. Radiol. Prot.* **38** 61–80
- [16] Harbron R W, Feltbower R G, Glaser A, Lilley J and Pearce M S 2014 Secondary malignant neoplasms following radiotherapy for primary cancer in children and young adults *Pediatr. Hematol. Oncol.* **31** 259–67
- [17] Darby S C *et al* 2013 Risk of ischemic heart disease in women after radiotherapy for breast cancer *New Engl. J. Med.* **368** 987–98
- [18] Taylor C *et al* (Early Breast Cancer Trialists’ Collaborative Group) 2017 Estimating the risks of breast cancer radiotherapy: evidence from modern radiation doses to the lungs and heart and from previous randomized trials *J. Clin. Oncol.* **35** 1641–9
- [19] Zhou L, Ming X, Zhang Y, Bai S and Deng J 2015 Imaging dose and cancer risk in image-guided radiotherapy of cancers *Med. Phys.* **93** S181–2
- [20] Zhang Y, Feng Y, Zhang Y, Ming X, Yu J, Carlson D J, Kim J and Deng J 2015 Is it the time for personalized imaging protocols in cancer radiation therapy? *Int. J. Radiat. Oncol. Biol. Phys.* **91** 659–60
- [21] Siiskonen T, Kaijaluo S and Florea T 2017 Imaging practices and radiation doses from imaging in radiotherapy *Phys. Med.* **42** 247–52
- [22] Wood T J, Davis A T and Earley J 2018 IPEM topical report: the first UK survey of dose indices from radiotherapy treatment planning computed tomography scans for adult patients *Phys. Med. Biol.* **63** 185008
- [23] Ding G X, Alaei P, Curran B, Flynn R, Gossman M, Mackie T R, Miften M, Morin R, Xu X G and Zhu T C 2018 Image guidance doses delivered during radiotherapy: quantification, management, and reduction: report of the AAPM Therapy Physics Committee Task Group 180 *Med. Phys.* **45** e84–e99
- [24] Martin C J, Harrison J D and Rehani M M 2020 Effective dose from radiation exposure in medicine: past, present, and future *Phys. Med.* **79** 87–92
- [25] Rogers D W O, Faddegon B A, Ding G X, MA C-M, We J and Mackie T R 1995 BEAM: a Monte Carlo code to simulate radiotherapy treatment units *Med. Phys.* **22** 503–24
- [26] Kawrakow I, Rogers D W O, Mainegra-Hing E, Tessier F, Townson R W and Walters B R B 2000 EGSnrc toolkit for Monte Carlo simulation of ionizing radiation transport (<https://doi.org/10.4224/40001303>)
- [27] Abuhaimeid A, Martin C J, Sankaralingam M, Gentle D J and McJury M 2014 An assessment of the efficiency of methods for measurement of the computed tomography dose index (CTDI) for cone beam (CBCT) dosimetry by Monte Carlo simulation *Phys. Med. Biol.* **59** 6307–26
- [28] Abuhaimeid A and Martin C J 2018 Evaluation of coefficients to derive organ and effective doses from cone-beam CT (CBCT) scans: a Monte Carlo study *J. Radiol. Prot.* **38** 189–206
- [29] Martin C J, Abuhaimeid A and Lee C 2021 Dose quantities for measurement and comparison of doses to individual patients in computed tomography (CT) *J. Radiol. Prot.* **41** 792–808
- [30] Kawrakow I and Walters B R B 2006 Efficient photon beam dose calculations using DOSXYZnrc with BEAMnrc *Med. Phys.* **33** 3046–56
- [31] Walters B, Kawrakow I and Rogers D W O 2021 DOSXYZnrc users manual *NRCC Report PIRS–794revB* (Ottawa: Ionizing Radiation Standards National Research Council of Canada)
- [32] Lee C, Lodwick D, Hurtado J, Pafundi D, Williams J L and Bolch W E 2010 The UF family of reference hybrid phantoms for computational radiation dosimetry *Phys. Med. Biol.* **55** 339–63
- [33] Lee C, Lamart S and Moroz B E 2013 Computational lymphatic node models in pediatric and adult hybrid phantoms for radiation dosimetry *Phys. Med. Biol.* **58** N59–N82
- [34] Geyer A M, O’Reilly S, Lee C, Long D J and Bolch W E 2014 The UF/NCI family of hybrid computational phantoms representing the current US population of male and female children, adolescents, and adults—application to CT dosimetry *Phys. Med. Biol.* **59** 5225–42
- [35] NCI 2020 Ncidose/Phantoms (available at: <https://ncidose.cancer.gov/#phantoms>) (Accessed 31 March 2022)
- [36] ICRP 2009 Adult reference computational phantoms. ICRP Publication 110 *Ann. ICRP* **39**
- [37] Parsons D and Robar J L 2016 Volume of interest CBCT and tube current modulation for image guidance using dynamic kV collimation *Med. Phys.* **43** 1808–17
- [38] Spezi E, Downes P, Radu E and Jarvis R 2009 Monte Carlo simulation of an x-ray volume imaging cone beam CT unit *Med. Phys.* **36** 127–36
- [39] Marchant T E and Joshi K D 2017 Comprehensive Monte Carlo study of patient doses from cone-beam CT imaging in radiotherapy *J. Radiol. Prot.* **37** 13–30
- [40] ICRP 2017 Diagnostic reference levels in medical imaging. ICRP Publication 135 *Ann. ICRP* **46**